J|A|C|S
COMMUNICATIONS

Published on Web 00/00/0000

High Affinity, Paralog-Specific Recognition of the Mena EVH1 Domain by a Miniature Protein

Dasantila Golemi-Kotra,[†] Rachel Mahaffy,[‡] Matthew J. Footer,[§] Jennifer H. Holtzman,[‡] Thomas D. Pollard,[‡] Julie A. Theriot,[§] and Alanna Schepartz*,[†,‡]

Departments of Chemistry and Molecular, Cellular, and Developmental Biology, Yale University, New Haven, Connecticut 06511, and Department of Biochemistry, Stanford University School of Medicine, Stanford, California 94305

Received August 15, 2003; E-mail: alanna.schepartz@yale.edu

EVH1 domains are found within a large number of multidomain signaling proteins that regulate the dynamics of the actin cytoskeleton, including those where external stimuli regulate cellular motility, shape, and adhesion.[1] Examples include *Drosophila* Enabled (Ena)[2] and its mammalian counterparts Mena,[1a] vasodilator-stimulated phosphoprotein (VASP),[3] Enabled/VASP-like protein (Evl),[1a] and Wiskott−Aldrich syndrome protein (WASP).[4] EVH1 domains regulate actin filament dynamics through interactions with cytoskeleton-associated proteins including vinculin and zyxin, and are used by the ActA protein of *Listeria monocytogenes* during pathogenesis.[5] Like SH3 and WW domains, EVH1 domains recognize proline-rich sequences on target proteins[6] that are folded into type II polyproline (PPII) helices.[7] In the case of *L. monocytogenes*, the interaction of intracellular EVH1 domains with ActA contributes to the propulsion of the bacterium through the host cell cytoplasm and into neighboring cells.[8]

Previously we described a miniature protein design strategy in which the well-folded helix in avian pancreatic polypeptide (aPP) presents short α-helical recognition epitopes (Figure 1A).[10,11] The miniature proteins so designed recognize even shallow clefts on protein surfaces with nanomolar affinities and high specificity.[11] aPP consists of an eight-residue PPII helix linked through a type I β-turn to a 20-residue α-helix. Here we extend this protein design strategy to stabilize the functional epitope of ActA on the PPII helix of aPP. Like miniature proteins that use an α-helix for protein recognition, the miniature protein designed in this way displays high affinity for the $Mena_{1-112}$ EVH1 domain and achieves the elusive goal of paralogue specificity,[12] discriminating well between EVH1 domains of $Mena_{1-112}$, $VASP_{1-115}$, and Evl_{1-115}.

Our design began with the structure of $Mena_{1-112}$ in complex with the proline-rich peptide $F_1P_2PP_4P_5$ (FP_4).[13] The structure shows the pentapeptide bound as a type II polyproline helix, with residues P_2, P_4, and P_5 nestled into the concave, V-shaped, binding surface on $Mena_{1-112}$, and residue F_1 anchoring the peptide in the N-to-C direction.[13] Substitution of FP_4 residues F_1, P_2, and P_5 at positions S_3, Q_4, and Y_7 of aPP, and extension of this core sequence by two of three C-terminal acidic residues shown to improve affinity and specificity,[13,14,5c] led to the final sequence of pGolemi (Figure 1B).

pGolemi was synthesized using standard solid-phase methods[9] and examined by circular dichroism (CD) spectroscopy (Figure 1C). The CD spectrum of pGolemi at 25 °C exhibited minima at approximately 208 and 222 nm, as expected for a protein containing one or more α-helices, and was independent of concentration between 5 and 20 μM. The mean residue ellipticity (Θ_{MRE}) at 222 nm of −13 979 deg·cm^2·dmol^{-1} suggests that approximately 13 residues of pGolemi possessed an α-helical conformation. The stability of pGolemi was examined further by monitoring the temperature-dependence of Θ_{MRE} at 222 nm. pGolemi underwent a reversible, moderately cooperative melting transition with T_m = 40 °C (Figure 1D). These data suggest that pGolemi adopts a moderately stable, folded, aPP-like structure.

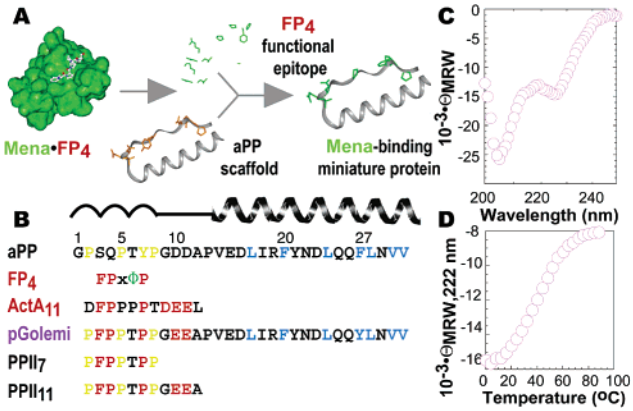

Figure 1. (A) Strategy for display of the FP_4 epitope on a miniature protein scaffold. (B) Sequences of peptides and miniature proteins described in this work. Residues important for aPP folding are in blue or yellow, residues important for $Mena_{1-112}$ recognition are in red. (C and D) CD spectra showing (C) the mean residue ellipticity (Θ_{MRE}) of 5 μM pGolemi at 25 °C and (D) the temperature dependence of the Θ_{MRE} at 222 nm.[9]

The affinity and specificity of pGolemi·EVH1 domain interactions were measured by tryptophan perturbation analysis (Figure 2A).[13] An 11-residue peptide comprising PPII repeat 1 of *L. monocytogenenes* ActA ($ActA_{11}$) and two peptides comprising the N-terminal 7 or 11 residues in pGolemi ($PPII_7$ and $PPII_{11}$) were prepared as controls. pGolemi bound $Mena_{1-112}$ with high affinity (K_d = 700 ± 30 nM).[9] This affinity is 10-fold higher than that of $ActA_{11}$, the best previously known Mena ligand.[13] The interaction between pGolemi and $Mena_{1-112}$ was confirmed by fluorescence polarization experiments using a fluorescent pGolemi derivative ($pGolemi^{Flu}$) (Figure 2B); the K_d determined this way was 290 ± 50 nM. Furthermore, pGolemi and $ActA_{11}$ compete with $pGolemi^{Flu}$ for binding to $Mena_{1-112}$ with IC_{50} values of 542 ± 30 nM and 4.0 ± 0.2 μM, respectively.[9] Interestingly, $PPII_7$ and $PPII_{11}$ were poor $Mena_{1-112}$ ligands (K_d = 480 μM and > 1 mM, respectively), indicating that the pGolemi α-helix contributes at least 3.5 kcal·mol^{-1} to the $Mena_{1-112}$ affinity of pGolemi.

The folded structure of pGolemi also contributes to its ability to differentiate EVH1 domain paralogs in vitro (Figure 2C). The sequences of EVH1 domains $Mena_{1-112}$, $VASP_{1-115}$, and Evl_{1-115} are 60% identical, and their structures are virtually superimposable.[14] Although $ActA_{11}$ binds equally to all EVH1 domains tested

[†] Department of Chemistry, Yale University.
[‡] Department of Molecular, Cellular and Developmental Biology, Yale University.
[§] Department of Biochemistry, Stanford University School of Medicine.

10.1021/ja037954k CCC: $27.50

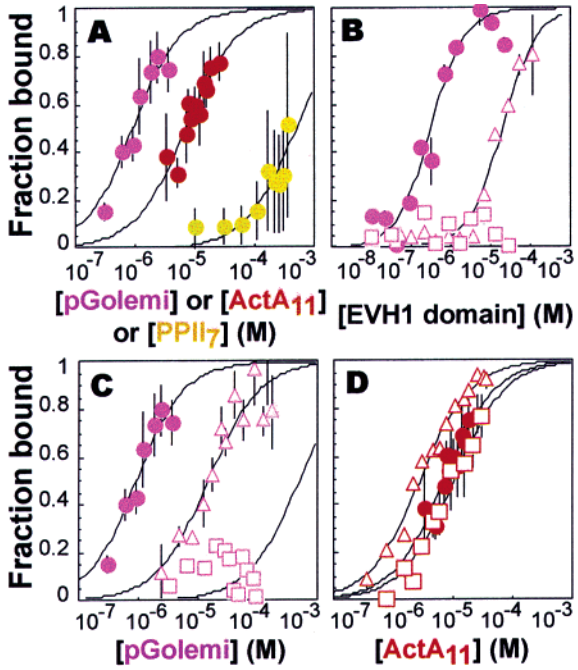

Figure 2. EVH1 domain binding interactions measured by tryptophan perturbation analysis (A, C, and D) or fluorescence polarization (B). (A) Binding of pGolemi (magenta), $ActA_{11}$ (red), or $PPII_7$ (yellow) to $Mena_{1-112}$ (500 nM). (B) Binding of $pGolemi^{Flu}$ (25 nM) to $Mena_{1-112}$ (circle), $VASP_{1-115}$ (triangle) or Evl_{1-115} (square). (C) Binding of pGolemi to $Mena_{1-112}$ (500 nM, circle), $VASP_{1-115}$ (500 nM, triangle), or Evl_{1-115} (500 nM, square). (D) Binding of $ActA_{11}$ to $Mena_{1-112}$ (500 nM, circle), $VASP_{1-115}$ (500 nM, triangle), or Evl_{1-115} (500 nM, square).[9] Fraction bound refers to the fraction of EVH1 domain (A, C, D) or $pGolemi^{Flu}$ (B) bound.

(Figure 2D, $K_{rel} < 3$), pGolemi prefers $Mena_{1-112}$ to $VASP_{1-115}$ ($K_{rel} = 20$) and especially to Evl_{1-115} ($K_{rel} > 120$) (Figure 2C). This level of specificity was confirmed by fluorescence polarization analysis (Figure 2B). pGolemi also discriminated well between $Mena_{1-112}$ and proteins that recognize proline-rich sequences or α-helices. The affinity of pGolemi for the KIX domain of CBP, which recognizes an α-helical ligand, was 15 ± 0.7 μM, and no interaction was detected between pGolemi and the N- or C-terminal SH3 domains of Grb-2.[9]

The properties of pGolemi were also examined in *Xenopus laevis* egg cytoplasmic extracts to reconstitute *L. monocytogenes* actin-based motility (Figure 3).[15] *L. monocytogenes* motility in mammalian cells and extracts is due to interactions between the 639-residue bacterial protein ActA and host proteins that recruit and activate actin polymerization. Addition of 10 μM $ActA_{11}$ decreased the median speed of *L. monocytogenes* by 89%, consistent with previous work.[16,5b] Addition of 10 or 27 μM pGolemi decreased the median speed of *L. monocytogenes* by 68% (Figure 3A) but, in addition, caused extreme speed variations and discontinuous tail formation at all times (Figure 3C). Discontinuous tails were not observed at any concentration of $ActA_{11}$ tested (Figure 3D). The differential effects of $ActA_{11}$ and pGolemi on *L. monocytogenes* motility may reflect their degree of specificity for EVH1 domain paralogs.

Many protein−protein interactions in cell signaling demand recognition of proline rich sequences,[6] and the design of molecules that perturb signaling pathways represents a foremost goal of chemical biology. Our results suggest that miniature proteins based on aPP may represent an excellent framework for the design of ligands that differentiate the roles of EVH1 domains in vitro and in vivo.

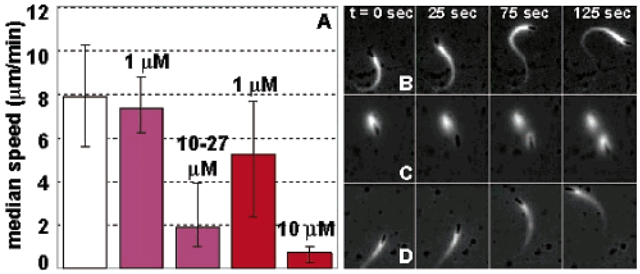

Figure 3. (A) Plot of median speed of *L. monocytogenes* observed in the absence (white) or presence (purple) of pGolemi and $ActA_{11}$ (red). Errors bars show the intraquartile range. (B−D) Time series of phase contrast and fluorescence micrographs of *L. monocytogenes* movement in a *Xenopus* egg cytoplasmic extract supplemented with rhodamine-labeled actin to mark the tails: (B) no added peptide, (C) 27 μM pGolemi, and (D) 1 μM $ActA_{11}$.[9]

Acknowledgment. We are grateful to Wendell Lim (UCSF), Steven Almo (AECOM), and Thomas Jarchau (Insitut für Klinische Biochemie und Pathobiochemie) for plasmids encoding His-$Mena_{1-112}$, GST-Evl_{1-115}, and GST-$VASP_{1-115}$, respectively. J.H.H. is grateful to NSERC-Canada for a predoctoral fellowship. This work was supported by the NIH (GM 59843 to A.S. and AI 36929 to J.A.T.) and in part by a grant to Yale University, in support of A.S., from the Howard Hughes Medical Institute.

Supporting Information Available: Characterization of molecules described in this work; analysis of $pGolemi^{Flu}$ affinity and specificity and effect on *L. monocytogenes* motility (PDF). This material is available free of charge via the Internet at http://pubs.acs.org.

References

(1) (a) Gertler, F. B.; Niebuhr, K.; Reinhard, M.; Wehland, J.; Soriano, P. *Cell* **1996**, *87*, 227. (b) Haffner, C.; Jarchau, T.; Reinhard, M.; Hoppe, J.; Lohmann, S. M.; Walter, U. *EMBO J.* **1995**, *14*, 19. (c) Reinhard, M.; Halbrugge, M.; Scheer, U.; Wiegand, C.; Jockusch, B. M.; Walter, U. *EMBO J.* **1992**, *11*, 2063.
(2) Gertler, F. B.; Doctor, J. S.; Hoffmann, F. M. *Science* **1990**, *248*, 857.
(3) Halbrugge, M.; Walter, U. *Eur. J. Biochem.* **1989**, *185*, 41.
(4) Callebaut, I.; Cossart, P.; Dehoux, P. *FEBS Lett* **1998**, *441*, 181.
(5) (a) Reinhard, M.; Jouvenal, K.; Tripier, D.; Walter, U. *Proc. Natl. Acad. Sci. U.S.A.* **1995**, *92*, 7956. (b) Southwick, F. S.; Purich, D. L. *Proc. Natl. Acad. Sci. U.S.A.* **1994**, *91*, 5168. (c) Niebuhr, K.; Ebel, F.; Frank, R.; Reinhard, M.; Domann, E.; Carl, U. D.; Walter, U.; Gertler, F. B.; Wehland, J.; Chakraborty, T. *EMBO J.* **1997**, *16*, 5433.
(6) Zarrinpar, A.; Bhattacharyya, R. P.; Lim, W. A. *Sci. STKE* **2003**, RE8.
(7) Williamson, M. P. *Biochem. J.* **1994**, *297*, 249.
(8) (a) Suarez, M.; Gonzalez-Zorn, B.; Vega, Y.; Chico-Calero, I.; Vazquez-Boland, J. A. *Cell Microbiol.* **2001**, *3*, 853. (b) Cameron, L. A.; Giardini, P. A.; Soo, F. S.; Theriot, J. A. *Nat. Rev. Mol. Cell. Biol.* **2000**, *1*, 110.
(9) See Supporting Information.
(10) (a) Zondlo, N. J.; Schepartz, A. *J. Am. Chem. Soc.* **1999**, *121*, 6938. (b) Chin, J. W.; Schepartz, A. *J. Am. Chem. Soc.* **2001**, *123*, 2929. (c) Chin, J. W.; Schepartz, A. *Angew. Chem., Int. Ed.* **2001**, *20*, 3806. (d) Chin, J. W.; Grotzfeld, R. M.; Fabian, M. A.; Schepartz, A. *Bioorg. Med. Chem. Lett.* **2001**, *11*, 1501. (e) Montclare, J. K.; Schepartz, A. *J. Am. Chem. Soc.* **2003**, *125*, 3416.
(11) Rutledge, S. E.; Volkmann, H.; Schepartz, A. *J. Am. Chem. Soc.* **2003**, *125*, 14336.
(12) Wong, J. C.; Hong, R.; Schreiber, S. L. *J. Am. Chem. Soc.* **2003**, *125*, 5586.
(13) Prehoda, K. E.; Lee, D. J.; Lim, W. A. *Cell* **1999**, *97*, 471.
(14) Ball, L. J.; Jarchau, T.; Oschkinat, H.; Walter, U. *FEBS Lett.* **2002**, *513*, 45.
(15) Theriot, J. A.; Fung, D. C. *Methods Enzymol.* **1998**, *298*, 114.
(16) Smith, G. A.; Theriot, J. A.; Portnoy, D. A. *J. Cell Biol.* **1996**, *135*, 647.

JA037954K